

Surface diffusion and low vibrational motion with interacting adsorbates: A shot noise description

R. Martínez-Casado^{a,c,*}, J. L. Vega^{b,c,†}, A. S. Sanz^{c,‡} and S. Miret-Artés^{c,§}

^a*Lehrstuhl für Physikalische Chemie I, Ruhr-Universität Bochum, D-44801 Bochum, Germany*

^b*Biosystems Group, School of Computing, University of Leeds, Leeds LS2 9JT, United Kingdom and*

^c*Instituto de Matemáticas y Física Fundamental,*

Consejo Superior de Investigaciones Científicas, Serrano 123, 28006 Madrid, Spain

(Dated: March 23, 2022)

Here, an approach in terms of shot noise is proposed to study and characterize surface diffusion and low vibrational motion when having interacting adsorbates on surfaces. In what we call *statistical limit*, that is, at long times and high number of collisions, one expects that diffusing particles display an essential Markovian behavior. Accordingly, the action of the pairwise potentials accounting for particle-particle collisions is equivalent to considering a shot noise acting on a single particle. We call this approach the *interacting single adsorbate approximation*, which gathers three important advantages: (i) the dynamics underlying surface diffusion and low vibrational motion can be easily understood in terms of relatively simple stochastic processes; (ii) from our model, appropriate (and well justified) working formulas are easily obtained, which explain the results arising from more complicated (but commonly used) molecular dynamics simulations within the Langevin formulation; and (iii), at the same time, it is less demanding computationally than the latter type of calculations. In order to illustrate the application of this model, numerical results are presented. Specially, our model reproduces the experimental observation regarding the broadening of the quasielastic peak ruling surface diffusion.

PACS numbers: 05.10.Gg, 05.40.-a, 68.43.-h

I. INTRODUCTION

Diffusion of adsorbates (e.g., atoms or small molecules) on metal surfaces is one of the most fundamental processes in surface science for which there is a wealth of available experimental data. These data are obtained by means of either standard time-of-flight techniques [1, 2, 3] or the more novel spin-echo measurements [4]. In both cases the theoretical approach followed to understand and explain the experimental results is basically the same. At low coverages [5] adsorbate-adsorbate interactions can be neglected; diffusion (*self-diffusion*) is well characterized by only studying the dynamics of a single adsorbate interacting with the surface. This approach is known as the *single adsorbate approximation*, where adsorbate dynamics are described by means of the (classical) standard Langevin equation, i.e., the diffusion process is considered as a Brownian-like motion [1, 2, 6, 7]. On the other hand, as the coverage increases, adsorbate-adsorbate interactions can no longer be neglected. In these cases, molecular dynamics techniques within the Langevin framework (MDL) are commonly used to study the problem to deal with the surface thermal vibrations. In this type of calculations the lateral dipole-dipole interaction between Na atoms as a function of the coverage is accounted for by pairwise potential functions. Previous

works [3, 8] using this approach have failed when trying to reproduce the experimental data quantitatively. However, recently it has been shown [9] that a good agreement with the experiment can be achieved by considering the adsorbate motion in three dimensions.

Introducing pairwise potential functions results in a realistic description of the adsorbate dynamics. However, there is not a simple manner to handle the resulting calculations by means of a theoretical model, and one can only proceed by using some suggested fitting functions. Moreover, employing MDL simulations always result in a relatively high computational cost due to the time spent by the codes in the evaluation of the forces among particles. This problem becomes worse when working with long-range interactions, since *a priori* they imply that one should consider a relatively large number of particles in order to obtain a good simulation. In such cases, one can also make use of truncations, as is commonly done when considering short-range interactions, but they might lead to serious inaccuracies [10]. Some alternative techniques have been proposed to overcome this drawback, though they are more expensive computationally.

In order to avoid such inconvenient (interpretative and computational) one can try to translate the behaviors observed in the experiment into a simple, realistic stochastic model. To achieve this goal, first note that when a few adsorbates are present on a surface, the single adsorbate approximation perfectly describes their dynamics [11]. For practical purposes, this means that long-range interactions can be assumed as negligible; otherwise, important effects would appear even when having adsorbates located at very far distances from each other. Hence, in principle, when having a higher coverage, one can assume

*Electronic address: ruth@imaff.cfmac.csic.es

†Electronic address: jlvega@imaff.cfmac.csic.es

‡Electronic address: asanz@imaff.cfmac.csic.es

§Electronic address: s.miret@imaff.cfmac.csic.es

that one adsorbate will basically feel the action of other adsorbates located in a certain neighborhood (as is corroborated by the calculations presented in Ref. [9], where only about 400 atoms were used in the simulations). In other words, the importance of the long-range tail of the particle-particle interaction becomes only relative. Now, in order to obtain a good simulation of a diffusion process, one has to consider very long times in comparison to the time scales associated to the friction caused by the surface or to the typical vibrational frequencies observed when the adsorbates keep moving inside a surface well. For example, in the Na/Cu(001) system the time scales associated to typical vibrational frequencies and frictions are of the order of a few picoseconds, while the propagation time employed in a typical MDL simulation is of the order of several nanoseconds [9]. This means that there will be a considerably large number of collisions during the time elapsed in the propagation, and therefore that at some point the past history of the adsorbate will be irrelevant. That is, adsorbates undergo so many collisions after some time that they lose any trace of the type of interaction among them when they are considered statistically. This memory loss is a signature of a Markovian dynamical regime, where adsorbates have reached what we call the *statistical limit*. Otherwise, for time scales relatively short, the interaction is not Markovian and it is very important to take into account the effects of the interactions on the particle and its dynamics (memory effects).

Based on the previous physical considerations, here we propose a numerical and analytical scheme to deal with the diffusion problem of interacting adsorbates as a function of the coverage. In particular, our scheme is framed within a Langevin formulation, and inspired by the theory of spectral-line collisional broadening developed by Van Vleck and Weisskopf [12] and the elementary kinetic theory of gases [13]. We call this approach the *interacting single adsorbate approximation*. The diffusion of a single adsorbate is modeled by a series of random pulses within a Markovian regime (i.e., pulses of relatively short duration in comparison with the system relaxation) simulating collisions between adsorbates. In particular, we describe these adsorbate-adsorbate collisions by means of a *white shot noise* [14] as a limiting case of colored shot noise. In this way, a typical MDL problem involving N adsorbates is substituted by the dynamics of a single adsorbate, where the action of the remaining $N - 1$ adparticles is replaced by a random force given by the shot noise. This type of noise has also been applied, for example, to study thermal ratchets [15] and mean first passage times [16]. A different type of collisional model has been recently used to obtain jump distributions [17]. A general account on colored noise can be found in [18].

Note that since our model faces the problem of adsorbate diffusion from a stochastic perspective, it is alternative to those other models that imply the use of MDL simulations. There are no incompatibilities between both approaches, stochastic and deterministic (“determinis-

tic” in the sense of how adsorbate-adsorbate interactions are handled), other than their respective ranges of validity. On the contrary, they complement each other, since the type of results rendered by our model could be used to better understand the behaviors and trends displayed by the fitting functions that appear in the latter.

The main goal in this work is to show that a lot of information about diffusion can be obtained by means of a simple stochastic model based on a shot noise. Thus, no substrate friction will be considered in our calculations. The combined action of two noises, Gaussian white noise to simulate the surface temperature and the white shot noise with a nonseparable interaction potential are tackled in a separate publication [19] (Hänggi and co-workers [15] have also used this combined scheme in the context of Brownian motors). In Sec. II we thus give a detailed account of the model that we propose here to simulate the interacting particle dynamics. Moreover, a discussion on the validity of the model is also provided in the light of the *fluctuation-dissipation theorem*. A brief account on the broadening of the quasielastic peak with coverage is provided in Sec. III. Numerical results for both flat and corrugated periodic surfaces (separable interaction potentials) are shown in Sec. IV as a function of the coverage, temperature, and ΔK . Finally, the main conclusions extracted from this work as well as a discussion on the range of validity of our model are given in Sec. V.

II. INTERACTING ADSORBATES AND SHOT NOISE

Particle motion under two-dimensional (2D) separable interaction potentials can be simplified as two independent 1D motions provided the correlations between the two components of the noise source along each direction can be neglected. Then, the motion of an adsorbate subjected to the action of a bath consisting of another adsorbates on a static 2D (separable) surface potential can be well described by a generalized Langevin equation

$$\ddot{x}(t) = - \int_0^t \gamma(t-t') \dot{x}(t') dt' + F[x(t)] + \delta R(t), \quad (1)$$

where x represents any of the two adsorbate degrees of freedom. In Eq. (1), $\gamma(t)$ is the bath memory function; $F = -\nabla V$ is the deterministic force, $V(x) = V(x+a)$ being a deterministic, phenomenological adiabatic potential accounting for the adsorbate-surface interaction at $T = 0$, with period a along the x direction; and $\delta R(t)$ is the stochastic force fluctuation, defined as

$$\delta R(t) \equiv R(t) - \langle\langle R \rangle\rangle, \quad (2)$$

with

$$\langle\langle R \rangle\rangle \equiv \sum_K P_K(\mathcal{T}) \langle R(t') \rangle_{\mathcal{T}}. \quad (3)$$

In this last expression, the double average bracket indicates the average over both number of collisions (K)

according to a certain distribution, P_K , and time (\mathcal{T}); the subscript \mathcal{T} denotes the average along the time interval \mathcal{T} . Note that both F and δR are forces per mass unit.

The random force $R(t)$ has the functional form of a shot noise,

$$R(t) = \sum_{k=1}^K b_k(t - t_k), \quad (4)$$

since it describes the collisions among the adsorbates. The information about the shape and effective duration of the k th adsorbate-adsorbate collision at t_k is thus provided by $b_k(t - t_k)$. According to the definition of a shot noise, the probability to observe K collisions after a time \mathcal{T} follows a Poisson distribution [14], given by

$$P_K(\mathcal{T}) = \frac{(\lambda \mathcal{T})^K}{K!} e^{-\lambda \mathcal{T}}, \quad (5)$$

where λ is the average number of collisions per time unit. Assuming sudden adsorbate-adsorbate collisions (i.e., strong but elastic collisions) and that after-collision effects relax exponentially at a constant rate λ' , the pulses in Eq. (4) can be modeled as

$$b_k(t - t_k) = c_k \lambda' e^{-\lambda'(t - t_k)}, \quad (6)$$

with $t - t_k > 0$ and c_k giving the intensity of the collision impact. Within a realistic model, collisions take place randomly at different orientations and energies. Hence it is reasonable to assume that the c_k coefficients follow an exponential law,

$$g(c_k) = \frac{1}{\alpha} e^{-c_k/\alpha}, \quad c_k \geq 0, \quad (7)$$

where the value of α will be determined later on. It can also be easily shown that this kind of distribution renders

the same results as considering the pulse intensity having the same value, C , for any collision. In such a case, wherever $\langle c_k \rangle$ and $\langle c_k^2 \rangle$ appear they have to be replaced by C and C^2 , respectively. Finally, we would like to mention that numerical tests using a different shape function (in particular, a Gaussian function) gives the same type of results.

Independently of their intensity, it is apparent from Eq. (6) that any pulse decays at the same rate λ' . This rate defines the decay time scale for collision events, $\tau_c = 1/\lambda'$. If τ_c is relatively small (i.e., collision effects relax relatively fast), the memory function in Eq. (1) will be local in time. This could be the case, for instance, of relatively dilute systems, where the average time between consecutive collisions is long enough in comparison to the energy transfer process that occurs during the collision. Then $\gamma(t - t') \simeq \gamma \delta(t - t')$ and the upper time limit can be extended to infinity. In doing so we obtain a standard Langevin equation

$$\ddot{x}(t) = -\lambda \dot{x}(t) + F[x(t)] + \delta R(t). \quad (8)$$

Here the friction coefficient γ measures the number of collisions per time unit, as λ in Eq. (5). Hence, from now on, we replace γ by λ . The collisional friction coefficient introduces a time scale $\tau_r = 1/\lambda$, which can be interpreted as the (average) time between two successive collisions. Thus, although each individual collision lasts for a time scale given by τ_c , its effects over the system take place in a time of the order of τ_r in getting damped.

In order to obtain some relevant information about the adsorbate diffusion process, it is important first to analyze the solutions of Eq. (8) and then to derive some average magnitudes of interest. The former are straightforwardly obtained by formal integration, this yielding

$$v(t) = v_0 e^{-\lambda t} + \int_0^t e^{-\lambda(t-t')} F[x(t')] dt' + \int_0^t e^{-\lambda(t-t')} \delta R(t') dt', \quad (9a)$$

$$x(t) = x_0 + \frac{v_0}{\lambda} (1 - e^{-\lambda t}) + \frac{1}{\lambda} \int_0^t [1 - e^{-\lambda(t-t')}] F[x(t')] dt' + \frac{1}{\lambda} \int_0^t [1 - e^{-\lambda(t-t')}] \delta R(t') dt', \quad (9b)$$

where $v_0 = v(0)$ and $x_0 = x(0)$. As can be seen, for $\delta R = 0$, Eqs. (9) are the formal solution of purely (dissipative) deterministic equations of motion. Hence, without loss of generality, they can be more conveniently expressed as

$$v(t) = v_d(t) + v_s(t), \quad (10a)$$

$$x(t) = x_d(t) + x_s(t), \quad (10b)$$

where d embraces the deterministic terms of the solutions

and s those other depending on the stochastic force. Note that when $\delta R \neq 0$ the deterministic part will also present some stochastic features due to the evaluation of $F(x)$ along $x(t)$.

Since $\langle \delta R(t) \rangle = 0$,

$$\langle v(t) \rangle = \bar{v}_d(t), \quad (11a)$$

$$\langle v^2(t) \rangle = \bar{v}_d^2(t) + \langle v_s^2(t) \rangle, \quad (11b)$$

$$\langle x(t) \rangle = \bar{x}_d(t), \quad (11c)$$

$$\langle x^2(t) \rangle = \bar{x}_d^2(t) + \langle x_s^2(t) \rangle, \quad (11d)$$

where the barred magnitudes indicate the respective averages of the deterministic part of the solution, and

$$\langle v_s^2(t) \rangle = e^{-2\lambda t} \int_0^t dt' e^{2\lambda t'} \int_{-t'}^{t-t'} e^{\lambda \tau} \mathcal{G}(\tau) d\tau, \quad (12a)$$

$$\begin{aligned} \langle x_s^2(t) \rangle &= \frac{1}{\lambda^2} \int_0^t dt' \left[1 - e^{-\lambda(t-t')} \right] \\ &\times \int_{-t'}^{t-t'} \left[1 - e^{-\lambda(t-t'-\tau)} \right] \mathcal{G}(\tau) d\tau. \end{aligned} \quad (12b)$$

In these expressions, $\mathcal{G}(\tau)$ is the time correlation function of the stochastic force,

$$\mathcal{G}(\tau) \equiv \langle \langle \delta R(t) \delta R(t') \rangle \rangle = \langle \langle \delta R(t) \delta R(t+\tau) \rangle \rangle \quad (13)$$

[the double bracket is defined as in Eq. (3)]. As seen in Eq. (12), $\mathcal{G}(\tau)$ is the same for both averages despite the time-dependent prefactors being different. Averaging over time implies that Eq. (13) is independent of time; average values and time-correlation functions will not depend specifically on the origin of time, but on the difference τ between two times considered. This condition defines the process as *stationary*.

A general expression for $\mathcal{G}(\tau)$ is readily obtained after straightforward algebraic manipulations to be

$$\mathcal{G}(\tau) = \frac{1}{\mathcal{T}} \sum_K P_K(\mathcal{T}) K \int_0^{\mathcal{T}} \langle b(t-t') b(t+\tau-t') \rangle_c dt', \quad (14)$$

where

$$\langle \cdot \rangle_c \equiv \int_0^\infty \cdot g(c) dc \quad (15)$$

is the average over the pulse intensity, with $g(c)$ given by Eq. (7). Taking into account that $\sum_K P_K(\mathcal{T}) K = \lambda \mathcal{T}$ and introducing the change of variable $\zeta = t-t'$, Eq. (14) can be approximated by

$$\mathcal{G}(\tau) = \lambda \int_{-\infty}^\infty \langle b(\zeta) b(\zeta + \tau) \rangle_c d\zeta, \quad (16)$$

which is a general expression independent of the pulse shape. This approximation relies on the hypothesis that $b(\zeta) \approx 0$ outside a narrow time interval $0 < \zeta < \Delta$, with Δ a few times larger than τ_c , but of the same order of magnitude. In particular, substituting Eq. (6) into Eq. (16) leads to

$$\mathcal{G}(\tau) = \frac{\lambda \lambda'}{\alpha^2} e^{-\lambda' |\tau|}. \quad (17)$$

By changing the order of the integration variables, integrating over t' , and taking advantage of the property $\mathcal{G}(-\tau) = \mathcal{G}(\tau)$, Eqs. (12) can be expressed as

$$\langle v_s^2(t) \rangle = \frac{2}{\alpha^2} \left\{ \frac{\lambda'}{2(\lambda' - \lambda)} (1 - e^{-2\lambda t}) - \frac{\lambda' \lambda}{\lambda'^2 - \lambda^2} [1 - e^{-(\lambda' + \lambda)t}] \right\}, \quad (18a)$$

$$\begin{aligned} \langle x_s^2(t) \rangle &= \frac{2}{\alpha^2} \left\{ \frac{t}{\lambda} - \frac{2\lambda' - \lambda}{(\lambda' - \lambda)\lambda^2} (1 - e^{-\lambda t}) + \frac{\lambda'}{2(\lambda' - \lambda)\lambda^2} (1 - e^{-2\lambda t}) \right. \\ &\quad \left. + \frac{1}{(\lambda' - \lambda)\lambda'} (1 - e^{-\lambda' t}) - \frac{1}{\lambda'^2 - \lambda^2} [1 - e^{-(\lambda' + \lambda)t}] \right\}. \end{aligned} \quad (18b)$$

In order to determine the value of α , we assume that $\lambda' \gg \lambda$, this rendering

$$\langle v_s^2(t) \rangle \approx \frac{1}{\alpha^2} (1 - e^{-2\lambda t}), \quad (19a)$$

$$\langle x_s^2(t) \rangle \approx \frac{1}{\alpha^2 \lambda^2} [2\lambda t + 1 - (2 - e^{-\lambda t})^2]. \quad (19b)$$

Moreover, when $t \rightarrow \infty$, we also assume that the equipartition theorem holds, and therefore

$$\frac{1}{2} m \langle v^2(\infty) \rangle = \frac{1}{2} k_B T. \quad (20)$$

Taking into account that $\bar{v}_d^2(t) = \bar{v}_0^2 e^{-2\lambda t}$ and that the

time-dependent term in Eq. (19a) vanish asymptotically, we obtain $\alpha = \sqrt{m/k_B T}$. On the other hand, if we consider that the system is initially thermalized (i.e., it follows a Maxwell-Boltzmann distribution in velocities) and has a uniform probability distribution in positions around $x = 0$, then $\bar{v}_0 = 0$, $\bar{v}_0^2 = k_B T/m$, and $\bar{x}_0 = 0$. Thus, for $\lambda' \gg \lambda$ (i.e., in the Poissonian white noise

limit), Eqs. (11) become

$$\langle v(t) \rangle = 0, \quad (21a)$$

$$\langle v^2(t) \rangle = \frac{k_B T}{m}, \quad (21b)$$

$$\langle x(t) \rangle = 0, \quad (21c)$$

$$\langle x^2(t) \rangle = \bar{x}_0^2 + \frac{k_B T}{m\lambda^2} \left[2\lambda t + 1 - \left(2 - e^{-\lambda t} \right)^2 \right]. \quad (21d)$$

These equations constitute a limit. Therefore, for values of the parameters out of the range of the approximation, deviations are expected. As will be seen, the behavior of the numerical results presented in Sec. IV fit fairly well the trends given by these equations, though λ' is not much larger than λ purposely. For example, for high values of λ , the equilibrium thermal velocity is given by $2f/\alpha^2$, with $f = \lambda'/2(\lambda' + \lambda)$, instead of $1/\alpha^2$ [note that if $\lambda' = r\lambda$, then $f = r/2(1 + r)$, which approaches $1/2$ when $r \rightarrow \infty$].

After using the approximation $\lambda' \gg \lambda$, Eqs. (21) coincide with those obtained for a Brownian motion. This is because within this approximation the shot noise behaves as a (Poissonian) white noise, displaying a behavior analogous to that of a Gaussian white noise (Brownian motion) whenever the number of collisions per time unit (λ) is very high and/or the total propagation time (\mathcal{T}) considered is sufficiently long. Note that in the limit where the number of collisions goes to infinity, the Poissonian distribution approaches a Gaussian one because of the central limit theorem.

As happens for pure Brownian motion ($V = 0$), two regimes are clearly distinguishable from Eqs. (21) when comparing λ and t . For $\lambda t \ll 1$, collision events are rare and the adparticle shows an almost free motion with relatively long mean free paths. This is the *ballistic* or *free-diffusion regime*, characterized by

$$\langle x^2(t) \rangle \sim \frac{k_B T}{m} t^2. \quad (22)$$

On the other hand, for $\lambda t \gg 1$, there is no free diffusion since the effects of the stochastic force (collisions) are dominant. This is the *diffusive regime*, where mean square displacements are linear with time, i.e., they follow *Einstein's law*,

$$\langle x^2(t) \rangle \sim \frac{2k_B T}{m\lambda} t = 2Dt. \quad (23)$$

In analogy to Brownian motion, from this last expression we also note for systems driven by a shot noise that (1) lowering the density of the particle gas (or, equivalently, λ) leads to a faster diffusion (the diffusion coefficient D increases), and (2) the latter becomes more active when the gas is heated.

Apart from the averages given above, it is also meaningful to compute the velocity autocorrelation function,

$$\mathcal{C}(\tau) \equiv \langle v(0) v(\tau) \rangle \equiv \lim_{\mathcal{T} \rightarrow \infty} \frac{1}{\mathcal{T}} \int_0^{\mathcal{T}} v(t) v(t + \tau) dt, \quad (24)$$

where the correlation time, which provides information about the line shape broadening (see Sec. III), is

$$\tilde{\tau} \equiv \frac{1}{\langle v_0^2 \rangle} \int_0^\infty \mathcal{C}(\tau) d\tau. \quad (25)$$

The velocity autocorrelation function can also be expressed as

$$\begin{aligned} \mathcal{C}(\tau) &= \langle v(t) v(t + \tau) \rangle \\ &= e^{-2\lambda t - \lambda \tau} \int_0^t dt' e^{2\lambda t'} \int_{-t'}^{t+\tau-t'} e^{\lambda s} \mathcal{G}(s) ds. \end{aligned} \quad (26)$$

Introducing Eq. (17) into the right hand side of the second equality of Eq. (26), and in the limit of large t , we reach

$$\mathcal{C}(\tau) = \frac{k_B T}{m} \frac{\lambda'^2 \lambda}{\lambda'^2 - \lambda^2} \left(\frac{e^{-\lambda \tau}}{\lambda} - \frac{e^{-\lambda' \tau}}{\lambda'} \right), \quad (27)$$

which in the limit $\lambda' \gg \lambda$ becomes

$$\mathcal{C}(\tau) = \frac{k_B T}{m} e^{-\lambda \tau}. \quad (28)$$

This expression has been derived starting from a colored shot noise. However, observe that it is identical to the velocity autocorrelation function corresponding to an Ornstein-Uhlenbeck process, the *only* stationary Gaussian diffusion process. This is because of the approximation used here: the number of collisions per time unit is very large. In this case, the central limit theorem applies and, according to *Doob's theorem*, the corresponding correlation function will display an exponential decay.

For $V \neq 0$, Eqs. (21) are expected to show some deviations at short time scales because of the role played by the terms corresponding to the deterministic force. This force leads to the presence of a confining potential, which makes the particles to move within a bound space region for a time. Hence the system will be more localized than in the free-potential case ($V = 0$) and there will be much less diffusion. Moreover, some in-phase correlations will also be apparent due to the particles that do not have energy enough to overcome the potential energy barrier. This gives rise to a nondiffusive type of motion. That is, a low frequency vibrational motion exerted by the so-called *frustrated translational mode* or *T mode*.

The velocity autocorrelation functions given by Eqs. (27) and (28) correspond to a dynamics ruled by completely flat surface. Physically, this would be the case of a low corrugated surface, for which the static force is negligible in both directions. On the contrary, when the surface corrugation is important, effects mediated by the *T mode* are expected to manifest in the correlation function. An interesting example to examine is that of a harmonic oscillator, which can model at a first order of approximation the oscillating behavior associated to the *T mode*. In this case [6, 20]

$$\mathcal{C}(\tau) = \frac{k_B T}{m} e^{-\lambda \tau / 2} \left(\cos \omega \tau - \frac{\lambda}{2\omega} \sin \omega \tau \right), \quad (29)$$

where

$$\omega = \sqrt{\omega_0^2 - \frac{\lambda^2}{4}} \quad (30)$$

and ω_0 is the harmonic frequency; for a nonharmonic potential, ω_0 represents the corresponding approximate harmonic frequency. Equation (29) can also be written as

$$\mathcal{C}(\tau) = \frac{k_B T}{m} \frac{\omega_0}{\omega} e^{-\lambda\tau/2} \cos(\omega\tau + \delta), \quad (31)$$

with

$$\delta \equiv (\tan)^{-1} \left(\frac{\lambda/2}{\omega} \right). \quad (32)$$

Observe that Eq. (28) is easily recovered in the limit $\omega_0 \rightarrow 0$ from either Eq. (29) or Eq. (31).

Finally, a brief discussion on the validity of Eq. (8) is worthy. As said above, this equation can only be used rigorously when having a *white noise*, i.e., when $\mathcal{G}(\tau) \sim \delta(\tau)$ and the memory function can be substituted by a constant. Otherwise, with colored noise, one has to use the generalized Langevin equation (1) [18]. According to the fluctuation-dissipation theorem [21], the friction in the Langevin equation is related to the fluctuations of the random force. This is formally expressed by the relationship between the frequency spectrum of the memory function and the random force correlation function,

$$\gamma(\omega) = \frac{m}{k_B T} \int_0^\infty \mathcal{G}(\tau) e^{-i\omega\tau} d\tau. \quad (33)$$

Introducing Eq. (17) into Eq. (33) yields

$$\gamma(\omega) = \lambda \frac{\lambda'}{\lambda' + i\omega}, \quad (34)$$

whose real part is

$$\text{Re}[\gamma(\omega)] = \frac{1}{2} [\gamma(\omega) + \gamma^*(\omega)] = \lambda \frac{\lambda'^2}{\lambda'^2 + \omega^2}. \quad (35)$$

Two limits are interesting in this expression: $\lambda' \ll \omega$ and $\lambda' \gg \omega$. The first limit involves very short time scales (smaller than τ_c), where the particularities of the adsorbate-adsorbate interaction potential have to be taken into account (for example, pairwise interaction), and therefore a MDL prescription has to be followed. In this case, Eq. (34) can be written as

$$\gamma(\omega) \approx \lambda \frac{\lambda'^2}{\omega^2}, \quad (36)$$

and hence the standard Langevin equation can no longer be used. Moreover, as a consequence, since the frequency depends on the friction the relaxation time scale τ_r is not well defined. Conversely, in the second case, the collision

time scale rules the system dynamics, since it establishes a (frequency) cutoff. This leads to

$$\gamma(\omega) \approx \lambda \left(1 - \frac{\omega^2}{\lambda'^2} \right) \quad (37)$$

which can be written as $\gamma(\omega) \sim \lambda$ [notice that $\lambda \equiv \gamma(0)$] whenever $\lambda \ll \omega \ll \omega_c = \tau_c^{-1}$. As can be seen, in this limit (which can also be written as $\tau_c \ll \tau_r$), the use of a standard Langevin equation is well justified. This limit holds for strong but localized (or instantaneous) collisions (as assumed here) as well as for weak but continuous interactions (Brownian motion).

III. ELEMENTS OF SURFACE DIFFUSION

In diffusion experiments carried out by means of quasielastic helium atom surface scattering (QHAS), one usually measures the *differential reflection coefficient*. In analogy to liquids [22] this magnitude is given as

$$\begin{aligned} \frac{d^2 \mathcal{R}(\Delta \mathbf{K}, \omega)}{d\Omega d\omega} &= n_d \mathcal{F} S(\Delta \mathbf{K}, \omega) \\ &= n_d \mathcal{F} \iint G(\mathbf{R}, t) e^{i(\Delta \mathbf{K} \cdot \mathbf{R} - \omega t)} d\mathbf{R} dt. \end{aligned} \quad (38)$$

This expression is the probability that the probe (He) atoms scattered from the diffusing collective (chattered on the surface) reach a certain solid angle Ω with an energy exchange $\hbar\omega = E_f - E_i$ and wave vector transfer parallel to the surface $\Delta \mathbf{K} = \mathbf{K}_f - \mathbf{K}_i$. In Eq. (38), n_d is the (diffusing) surface concentration of adparticles; \mathcal{F} is the *atomic form factor*, which depends on the interaction potential between the probe atoms in the beam and the adparticles on the surface; and $S(\Delta \mathbf{K}, \omega)$ is the *dynamic structure factor* or *scattering law*, which provides a complete information about the dynamics and structure of the adsorbates through particle distribution functions. The dynamic structure factor is therefore the observable magnitude that we are interested in here. Experimental information about long distance correlations is obtained from it when using small values of $\Delta \mathbf{K}$, while information on long time correlations is available at small energy transfers, $\hbar\omega$. On the other hand, a standard procedure employed to obtain the adiabatic adsorption potential $V(\mathbf{R})$ mediating the adsorbate-substrate interaction consists in starting with a model potential that contains some adjustable parameters. Then, Markovian-Langevin equations are solved for different friction coefficients with Gaussian white noise to reproduce the experimental QHAS measurements [2].

When dealing with interacting particles, particle distribution functions are described by means of the so-called van Hove or time-dependent pair correlation function $G(\mathbf{R}, t)$ [22]. Given a particle at the origin at some arbitrary initial time, $G(\mathbf{R}, t)$ represents the average probability for finding the same or another particle at the

surface position $\mathbf{R} = (x, y)$ at time t . This function thus generalizes the well known pair distribution function $g(\mathbf{R})$ from statistical mechanics [13, 23], since it provides information about the interacting particle dynamics. Depending on whether we consider correlations of a particle with itself or with other different particles, we distinguish between *self* correlation functions, $G_s(\mathbf{R}, t)$, and *distinct* correlation functions, $G_d(\mathbf{R}, t)$, respectively. With this, the full (classical) pair correlation function can be expressed as

$$G(\mathbf{R}, t) = G_s(\mathbf{R}, t) + G_d(\mathbf{R}, t). \quad (39)$$

According to its definition, $G_s(\mathbf{R}, t)$ is peaked at $t = 0$, and approaches zero as t increases since the particle loses correlation with itself. On the other hand, at $t = 0$, $G_d(\mathbf{R}, t)$ gives the static pair correlation function (the standard pair distribution function), $g(\mathbf{R}) \equiv G_d(\mathbf{R}, 0)$, while approaches the mean surface number density σ of diffusing particles as $t \rightarrow \infty$. Taking this into account, Eq. (39) can be expressed as

$$G(\mathbf{R}, 0) = \delta(\mathbf{R}) + g(\mathbf{R}) \quad (40)$$

at $t = 0$, and as

$$G(\mathbf{R}, t) \approx \sigma \quad (41)$$

for a homogeneous system with $\|\mathbf{R}\| \rightarrow \infty$ and/or $t \rightarrow \infty$. At low adparticle concentrations, when interactions among adsorbates can be neglected because they are far apart from each other, the main contribution to Eq. (39) is G_s (particle-particle correlations are negligible and $G_d \approx 0$). On the contrary, for high coverages, it is expected that G_d contributes significantly to Eq. (39). Within our approach, the interaction among adsorbates is described by a particle subjected to a random force (a shot noise). Thus, diffusion is described by the $G = G_s$ function in the *interacting single adsorbate approximation*. At low coverages, the G_s function in both approximations (interacting and noninteracting) has to be the same.

As seen in Sec. II, although Gaussian white noise arising from the surface is not considered here, an analogous Markovian-Langevin also emerges from our model based on shot noise. Therefore the same analytical results obtained elsewhere [6] with a Gaussian white noise can be easily extended to our case, where the friction coefficient has to be interpreted in terms of the collision frequency between adsorbates. For this treatment, the dynamic structure factor is better expressed as [22]

$$\begin{aligned} S(\Delta\mathbf{K}, \omega) &= \int e^{-i\omega t} \langle e^{-i\Delta\mathbf{K} \cdot \mathbf{R}(t)} e^{i\Delta\mathbf{K} \cdot \mathbf{R}(0)} \rangle dt \\ &= \int e^{-i\omega t} I(\Delta\mathbf{K}, t) dt, \end{aligned} \quad (42)$$

where the brackets in the integral denote an ensemble average and $\mathbf{R}(t)$ is the adparticle trajectory. Here,

$$I(\Delta\mathbf{K}, t) \equiv \langle e^{-i\Delta\mathbf{K} \cdot [\mathbf{R}(t) - \mathbf{R}(0)]} \rangle = \langle e^{-i\Delta\mathbf{K} \cdot \int_0^t \mathbf{v}\mathbf{K}(t') dt'} \rangle \quad (43)$$

is the *intermediate scattering function*, which is the space Fourier transform of $G(\mathbf{R}, t)$ [24]. In Eq. (43), $v_{\Delta\mathbf{K}}$ is the velocity of the adparticle projected onto the direction of the parallel momentum transfer, with length $\Delta K \equiv \|\Delta\mathbf{K}\|$. After a second-order cumulant expansion in ΔK in the second equality of Eq. (43), the intermediate scattering function reads as

$$I(\Delta\mathbf{K}, t) \approx e^{-\Delta K^2 \int_0^t (t-t') \mathcal{C}(t') dt'}, \quad (44)$$

where $\mathcal{C}(t)$ is given by Eq. (24) [note that $\mathcal{C}(t)$, as given by Eq. (24), is independent of the direction of $\Delta\mathbf{K}$]. This is the so-called *Gaussian approximation* [13], which is exact when the velocity correlations at more than two different times are negligible. This allows one to replace the average acting over the exponential function in Eq. (43) by an average acting over its argument, as seen in Eq. (44).

In the case of an almost flat surface the resulting intermediate scattering function is

$$I(\Delta\mathbf{K}, t) = \exp[-\chi^2 (e^{-\lambda t} + \lambda t - 1)], \quad (45)$$

with

$$\chi^2 \equiv \langle v_0^2 \rangle \Delta K^2 / \lambda^2. \quad (46)$$

From this relation we can obtain both the mean free path, $\bar{l} \equiv \tau_r \sqrt{\langle v_0^2 \rangle}$, and the self-diffusion coefficient, $D \equiv \tau_r \langle v_0^2 \rangle$ (Einstein relation). It can be easily shown that the dynamic structure factor derived from Eq. (45) has a Gaussian shape for short times compared to $\tilde{\tau} = \tau_r$ (or $\chi \rightarrow \infty$) and a Lorentzian shape for long times or values of small ΔK (or $\chi \ll 1$) [6, 25]. In this last case, Eq. (45) becomes a pure decaying exponential function,

$$I(\Delta\mathbf{K}, t) \approx e^{-\chi^2 \lambda t}, \quad (47)$$

which is in agreement with the ansatz used in Ref. [9] to fit the polarization values obtained experimentally.

On the other hand, when a harmonic oscillator is considered, Eq. (44) becomes

$$I(\Delta\mathbf{K}, t) = \exp \left\{ -\frac{\chi^2 \lambda^2}{\omega \omega_0} \left[\cos \delta - e^{-\lambda t/2} \cos(\omega t - \delta) \right] \right\}. \quad (48)$$

As inferred from this equation, the intermediate scattering function displays an oscillatory, but exponentially damped, behavior around a certain value [although in the limit $\omega_0 \rightarrow 0$ Eq. (48) approaches Eq. (45)]. Unlike the free-potential case, this means that after relaxation some correlation is still present in the system, being the limit value

$$I(\Delta\mathbf{K}, \infty) \rightarrow e^{-\chi^2 \lambda^2 \cos \delta / \omega \omega_0}. \quad (49)$$

Again, this is in agreement with the experimental observation. According to Ref. [9] the residual or anomalous value of the polarization observed seems to be connected to the blockage of the adsorbate perpendicular motion (which is related to translational hopping). On

the other hand, according to our model, another source for such an effect could be that some Na atoms would become trapped inside potential wells, thus behaving as damped oscillators. Nonetheless, note that in both cases the anomalous behavior for $I(t)$ arises from inhibiting the free diffusion of the atoms on the surface. For realistic corrugated surfaces, one will find a nonseparable combination of this behavior (related to the trapped particles inside the potential wells) and that described by Eq. (45) (associated to the free-diffusing particles). The corresponding scattering law has been given elsewhere [6] for models where the velocity autocorrelation function can be expressed in terms of a damped anharmonic oscillator.

Taking into account the approximation for the intermediate scattering function, we can now relate in an easy manner the velocity power spectrum with the dynamic structure factor. As can be readily seen from Eq. (44) [23], we have

$$\mathcal{C}(t) = - \lim_{\Delta K \rightarrow 0} \frac{1}{\Delta K^2} \frac{d^2 I(\Delta \mathbf{K}, t)}{dt^2}, \quad (50)$$

where the velocity is recorded along the $\Delta \mathbf{K}$ direction. The velocity power spectrum or Fourier transform of the velocity autocorrelation function is defined as

$$Z(\omega) = \int_{-\infty}^{\infty} \mathcal{C}(t) e^{-i\omega t} dt. \quad (51)$$

Thus, by Fourier transforming both sides in Eq. (50) we obtain

$$Z(\omega) = \omega^2 \lim_{\Delta K \rightarrow 0} \frac{S(\Delta K, \omega)}{\Delta K^2}. \quad (52)$$

The interest in this expression relies on the fact that it allows us to obtain a relationship between the diffusion coefficient, D , and the full width at half maximum (FWHM) of S by setting $\omega = 0$ in Eq. (52), since

$$D = \frac{1}{2} Z(\omega = 0). \quad (53)$$

For example, for a Lorentzian-shaped S , the FWHM is given by $\Gamma = 2D\Delta K^2$, which is basically the line shape that one can observe in an experiment. On the other hand, if the line shape is Gaussian, its FWHM is $\Gamma = 2\sqrt{2 \ln 2} \langle v_0^2 \rangle^{1/2} \Delta K$.

Before concluding this section, we would like to give a brief account on how to relate in a simple manner the coverage θ and λ . In the elementary kinetic theory of transport in gases (see, for example, Ref. [13]), diffusion is proportional to the mean free path \bar{l} , which is proportionally inverse to both the density of gas particles and the effective area of collision when a hard-sphere model is assumed. For 2D collisions, the effective area is replaced by an effective length (twice the radius ρ of the adparticle) and the gas density by the surface density σ . With this, the mean free path reads as

$$\bar{l} = \frac{1}{2\sqrt{2}\rho\sigma}. \quad (54)$$

According to the Chapman-Enskog theory for hard spheres, the self-diffusion coefficient can be written as

$$D = \frac{1}{6\rho\sigma} \sqrt{\frac{k_B T}{m}}. \quad (55)$$

Now, from the Einstein relation, and taking into account that $\theta = a^2\sigma$ for a square surface lattice of unit cell length a , we obtain

$$\lambda = \frac{6\rho\theta}{a^2} \sqrt{\frac{k_B T}{m}}. \quad (56)$$

Therefore, given a certain surface coverage and temperature, λ can be readily estimated from Eq. (56).

IV. RESULTS AND DISCUSSION

A. Numerical details

In order to solve Eq. (8) we have used the velocity Verlet algorithm, which is commonly applied when dealing with stochastic differential equations [26]. For the average calculations shown here a number of 10 000–20 000 trajectories is sufficient for convergence. The initial conditions are chosen such that the velocities are distributed according to a Maxwell-Boltzmann velocity distribution at a temperature T , and the positions follow a uniform random distribution along the extension of a single unit cell of the potential model used (see below). Regarding the dynamical parameters, we have used $\lambda' = 10^{-3}$ a.u. (≈ 41.3 ps $^{-1}$) and for the mass and radius of the adparticles we have considered those of a Na atom, since Na on Cu(001) is a typical system where diffusion has been studied and will serve to illustrate our model numerically. As for the coverage, $\theta_{\text{Na}} = 1$ corresponds to one Na atom per Cu(001) surface atom or, equivalently, $\sigma = 1.53 \times 10^{19}$ atom/cm 2 [3]; $a = 2.557$ Å is the unit cell length; and $\rho = 2$ Å has been used for the atomic radius. For example, with these values a collision friction $\lambda = 5 \times 10^{-6}$ a.u. (≈ 0.2067 ps $^{-1}$) at a surface temperature $T = 100$ K would be related to a coverage $\theta_{\text{Na}} = 0.059$, while the same friction at a temperature $T = 200$ K would be caused by a coverage $\theta_{\text{Na}} = 0.042$. One order of magnitude higher for λ implies also one order of magnitude for the coverage at the corresponding surface temperatures.

B. Diffusion in a flat surface

First we are going to analyze the case of a flat surface, which represents fairly well the situation of a low corrugated real surface, where the role of the activation barrier is negligible. Thus, in Fig. 1(a) we observe that, effectively, as predicted by the theory, two (time) regimes are distinguishable from the mean square displacement

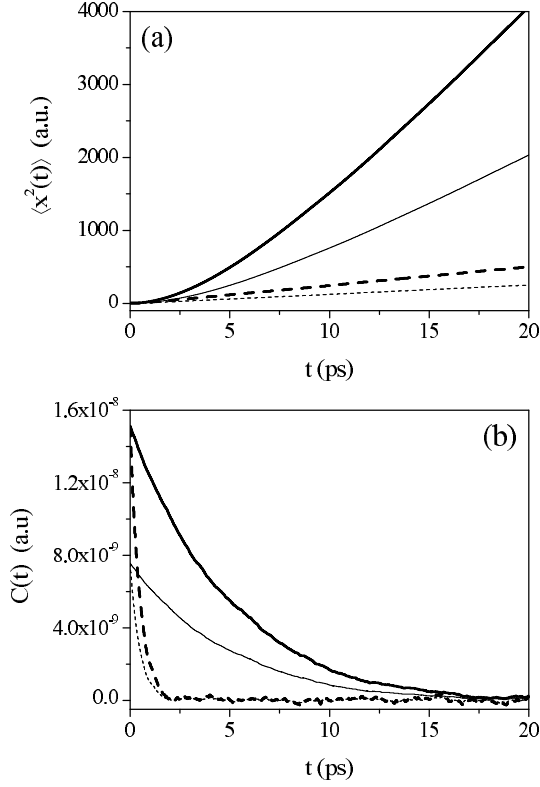


FIG. 1: (a) $\langle x^2(t) \rangle$ for two different temperatures and two values of the friction coefficient. (b) $\mathcal{C}(t)$ for the same temperatures and friction coefficients as in (a). The temperatures used are $T = 100$ K (thin lines) and $T = 200$ K (thick lines), and the friction coefficients are $\lambda = 5 \times 10^{-6}$ a.u. (solid lines) and $\lambda = 5 \times 10^{-5}$ a.u. (dashed lines).

$\langle x^2(t) \rangle$: parabolic and linear, corresponding to free and diffusive motion, respectively. As is apparent, diffusion (proportional to the slope of the linear regime) is enhanced by increasing temperature and decreasing the friction coefficient. Within the diffusive regime, though the presence of many particles tends to inhibit individual particle motions, there is still the possibility for particles to propagate but at a smaller rate [compare the quadratic increase of $\langle x^2(t) \rangle$ during the free motion with its linear increase during the diffusive one]. The effect of the diffusion process can also be seen by looking at the velocity autocorrelation function $\mathcal{C}(t)$ plotted in Fig. 1(b). As seen, the larger λ the faster the decay, this result being in agreement with Eq. (28) as well as its exponential decay. The numerical results fit perfectly on this decay, but with a slightly lower λ than the nominal one because, strictly speaking, ours is not a rigorous white shot noise. The agreement can also be observed when increasing the temperature, leaving λ unchanged; the starting value of $\mathcal{C}(t)$ increases, but its trend, $e^{-\lambda t}$, remains the same.

For a flat surface the Gaussian approximation assumed in Eq. (44) for $I(t)$ is exact. This is numerically corroborated by looking at the results presented in Fig. 2, where two different values of ΔK , 0.88 \AA^{-1} and 1.23 \AA^{-1} , are

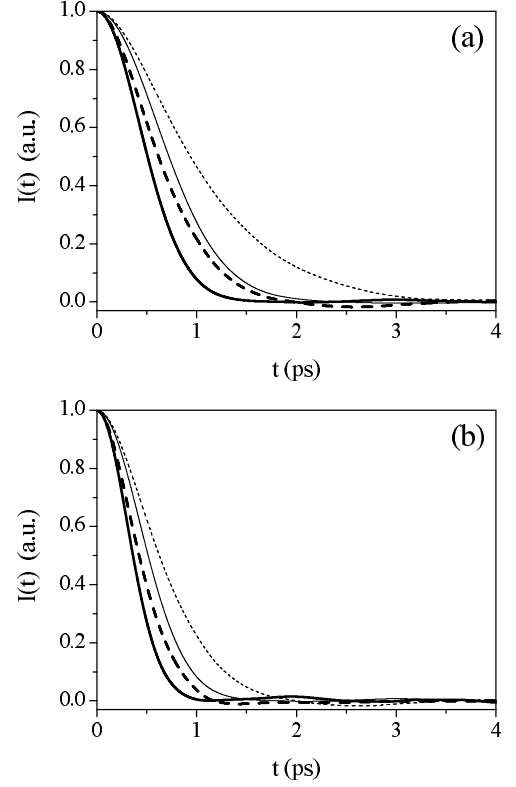


FIG. 2: (a) $I(t)$ for two different temperatures and two values of the friction coefficient, and $\Delta K = 0.88 \text{ \AA}^{-1}$. (b) Same as (a), but for $\Delta K = 1.23 \text{ \AA}^{-1}$. The temperatures used are $T = 100$ K (thin lines) and $T = 200$ K (thick lines), and the friction coefficients are $\lambda = 5 \times 10^{-6}$ a.u. (solid lines) and $\lambda = 5 \times 10^{-5}$ a.u. (dashed lines).

analyzed. As is apparent, for both ΔK values, the initial falloff of $I(t)$ displays a Gaussian shape, while for longer times it is exponential. This makes that the dynamic structure factor (see Fig. 3) at small positive (annihilation events) and negative (creation events) energy transfers, i.e., the quasielastic peak region, displays a mixed Gaussian-Lorentzian profile describable by using the Γ and incomplete Γ functions [6, 25]. Notice from these plots that as λ increases the line shape undergoes narrowing, unlike what one would expect when having collision events. This result for a flat surface, which is also predicted analytically, can be explained as follows. Noninteracting adsorbates behave like an ideal gas, i.e., particles spread out freely, without feeling the action of any other particle. This gives rise to dynamic structure factors that display Gaussian profiles. However, as particle-particle interactions are taken into account there is a friction arising from the neighboring adsorbates that opposes the free motion, which increases with increasing λ . That is, going back to the results presented in Fig. 1(a), the particle reaches the diffusive regime faster as λ becomes larger. The corresponding line shapes are no longer Gaussian functions and display narrowing at larger values of λ (see Fig. 3), as analytically predicted

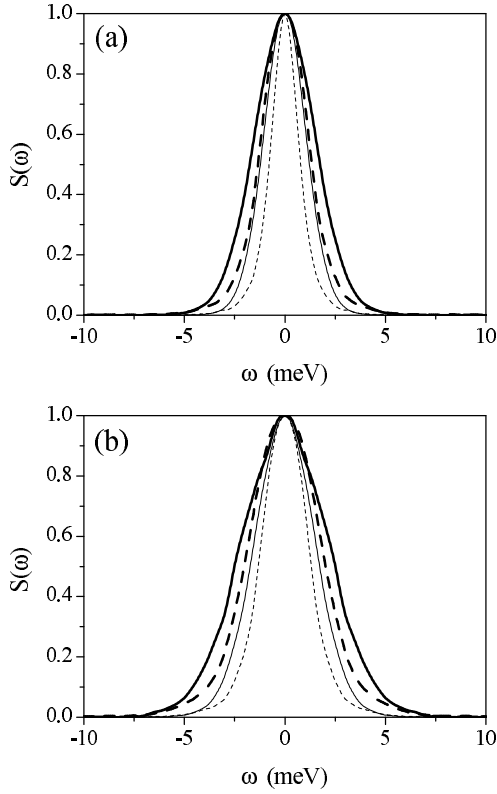


FIG. 3: (a) $S(\omega)$ for two different temperatures and two values of the friction coefficient, and $\Delta K = 0.88 \text{ \AA}^{-1}$. (b) Same as (a), but for $\Delta K = 1.23 \text{ \AA}^{-1}$. The temperatures used are $T = 100 \text{ K}$ (thin lines) and $T = 200 \text{ K}$ (thick lines), and the friction coefficients are $\lambda = 5 \times 10^{-6} \text{ a.u.}$ (solid lines) and $\lambda = 5 \times 10^{-5} \text{ a.u.}$ (dashed lines). In all cases, $S(\omega)$ has been normalized to unity in order to better appreciate the line shape broadening/narrowing; moreover, they have also been smoothed out to eliminate contributions coming from long-time fluctuations in $I(t)$.

by the scattering law [6, 25]. Of course, as temperature increases, for a fixed λ , one evidently observes the broadening of the line shape.

Finally, observe that the results presented here are similar to those that one would obtain with a Brownian-like motion: (i) with λ a slow diffusion is observed according to the Einstein relation, and (ii) diffusion becomes more active as the temperature of the ensemble of adparticles increases. However, also note that unlike a Brownian motion, diffusion appears here as a consequence of the discrete (in time) “kicks” felt by the particles. Moreover, between two consecutive “kicks” or collisions, they move basically without feeling any stochastic force (this is similar to the collision model proposed in Ref. [17]).

C. Diffusion in a separable potential

When the surface corrugation is relatively strong and cannot be neglected, it will induce very important effects

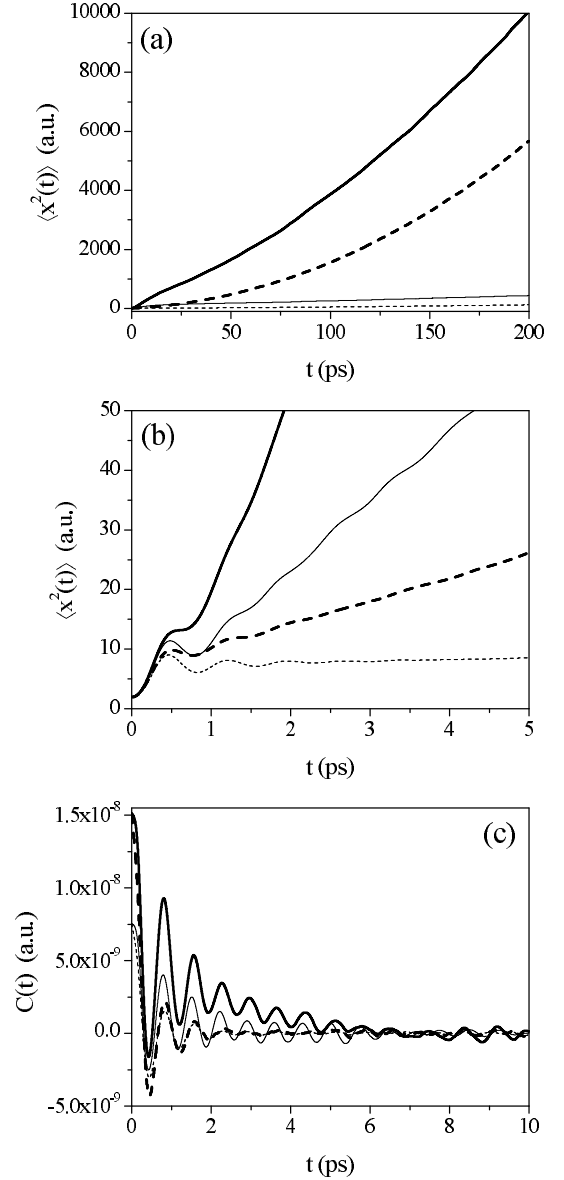


FIG. 4: (a) $\langle x^2(t) \rangle$ for two different temperatures and two values of the friction coefficient. (b) Enlargement at short times of part (a). (c) $C(t)$ for the same temperatures and friction coefficients as in (a). The temperatures used are $T = 100 \text{ K}$ (thin lines) and $T = 200 \text{ K}$ (thick lines), and the friction coefficients are $\lambda = 5 \times 10^{-6} \text{ a.u.}$ (solid lines) and $\lambda = 5 \times 10^{-5} \text{ a.u.}$ (dashed lines).

regarding the adsorbate dynamics. To illustrate these effects here we consider an adsorbate-surface interaction potential model

$$V(x, y) = V_0[2 - \cos(2\pi x/a) - \cos(2\pi y/a)], \quad (57)$$

where $2V_0 = 33.5 \text{ meV}$ is the activation barrier height in one direction (x or y). As a function of the temperature, the behavior is the same as previously observed for a flat surface. As can be seen in Fig. 4(a) [and in an enlargement view in Fig. 4(b)], for a given temperature

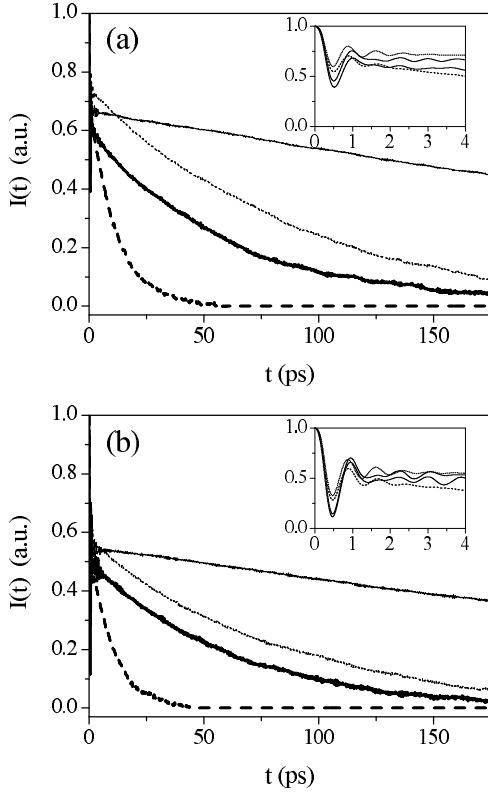


FIG. 5: (a) $I(t)$ for two different temperatures and two values of the friction coefficient, and $\Delta K = 0.88 \text{ \AA}^{-1}$. (b) Same as (a), but for $\Delta K = 1.23 \text{ \AA}^{-1}$. The temperatures used are: $T = 100 \text{ K}$ (thin lines) and $T = 200 \text{ K}$ (thick lines); and the friction coefficients are: $\lambda = 5 \times 10^{-6} \text{ a.u.}$ (solid lines) and $\lambda = 5 \times 10^{-5} \text{ a.u.}$ (dashed lines).

the presence of the potential also inhibits the diffusion of particles at larger values of λ since the number of them trapped in the potential wells is also larger (according to Einstein's law). This result is also reported in Refs. [3, 8] when the coverage increases. However, the effect of the static interaction potential will give rise to observing the opposite behavior than in the case of a flat surface: as λ increases line shapes become broader, a result which is also observed experimentally [3]. This is because now both motions, diffusion and vibration, are coupled. Thus, with increasing λ , the adsorbates can remain localized inside a given surface well for longer times. This allows one to observe a higher collisional damping in the T mode, which participates actively in the diffusion process. This is clearly depicted in Fig. 4(c), where the velocity autocorrelation function displays an oscillatory behavior, which is more damped as λ increases. We observe that $\mathcal{C}(t)$ fits the profile given by Eq. (31) but with parameters different from a harmonic oscillator (see Ref. [6] for an anharmonic oscillator model). Only for a motion localized mainly at the bottom of the potential well, the harmonic oscillator profile will be reproduced.

The oscillations due to the T mode are not only observable in a plot of $\mathcal{C}(t)$, but they also manifest in $I(t)$

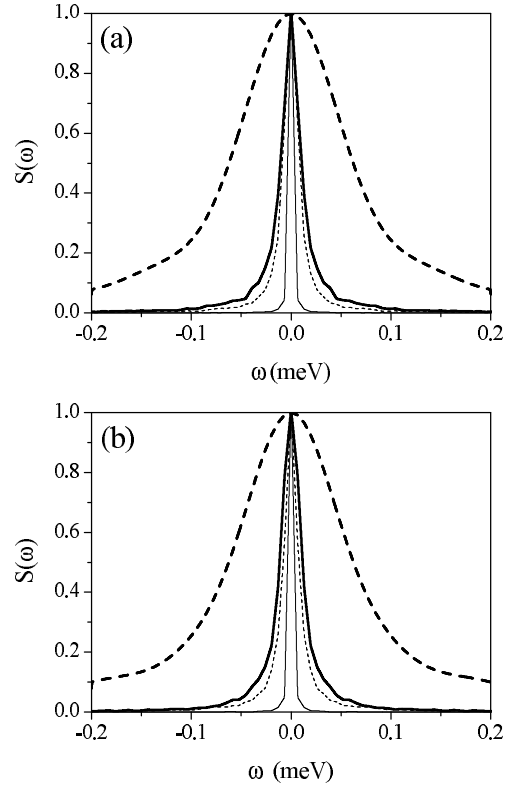


FIG. 6: (a) $S(\omega)$ for two different temperatures and two values of the friction coefficient, and $\Delta K = 0.88 \text{ \AA}^{-1}$. (b) Same as (a), but for $\Delta K = 1.23 \text{ \AA}^{-1}$. The temperatures used are: $T = 100 \text{ K}$ (thin lines) and $T = 200 \text{ K}$ (thick lines); and the friction coefficients are: $\lambda = 5 \times 10^{-6} \text{ a.u.}$ (solid lines) and $\lambda = 5 \times 10^{-5} \text{ a.u.}$ (dashed lines). In all cases, $S(\omega)$ has been normalized to unity in order to better appreciate the line shape broadening or narrowing; moreover, they have also been smoothed out to eliminate contributions coming from long-time fluctuations in $I(t)$.

(see Fig. 5) and $S(\omega)$ (see Fig. 6) for two values of ΔK , 0.88 \AA^{-1} and 1.23 \AA^{-1} , covering the region of the first Brillouin zone, $[0, 1.3] \text{ \AA}^{-1}$. As shown elsewhere [6], the FWHM of the quasielastic peak is quite similar for both ΔK values and therefore the variation obtained in the width is due only to the effect of λ . Plotting $I(t)$ we can observe a loss of phase when comparing this function for different values of λ . This behavior continues for all oscillations and ends up with $I(t)$ falling faster for the case with larger λ , thus given rise to broadening as λ increases. Nonetheless, it is expected that for relatively large values of λ , one can recover the behavior observed in the flat case.

Finally, in Fig. 7 the peak corresponding to the T mode placed around the frequency of oscillation (4 meV in energy) is plotted for the same two values of ΔK as before. Not only a shift of the position but also a broadening are clearly seen with λ , as also observed experimentally [3]. For both the quasielastic peak and the T mode peak the analytical formulas for the line shapes given elsewhere [6]

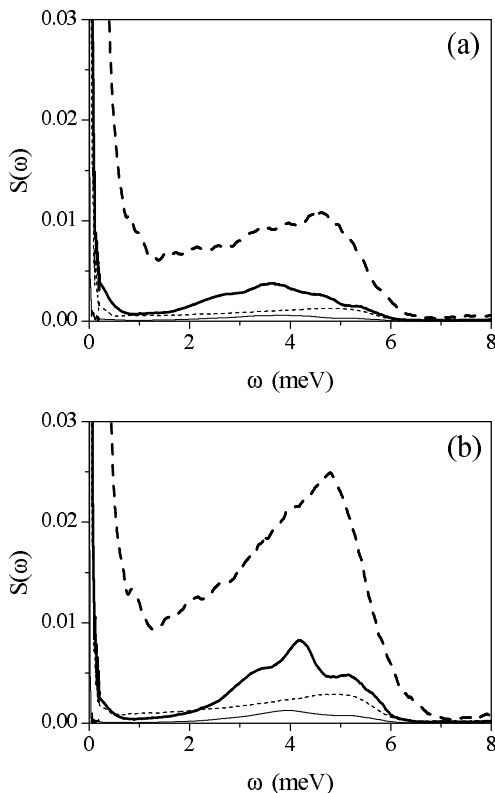


FIG. 7: Same as Fig. 6, but enlarged to show the peaks corresponding to the T mode. Since this mode is symmetric with respect to $\omega = 0$ meV, only the one located to the right of the quasielastic peak is shown in every case.

in the context of Gaussian white noise also fit fairly well the numerical results presented for the white shot noise model used here.

V. CONCLUSIONS

We would like to stress that the same treatment developed here for a separable 2D periodic potential can be easily generalized to a nonseparable 2D periodic surface with substrate friction due to a Gaussian white noise [19], this model describing the process in a more realistic fashion. In particular, preliminary results with the nonseparable 2D periodic surface for a low coverage ($\theta_{\text{Na}} = 0.028$) have rendered a value $\Gamma = 120 \mu\text{eV}$ for the quasielastic peak width at $\Delta K = 1.26 \text{ \AA}^{-1}$, which is in agreement with the experimental and theoretical values, $\Gamma_{\text{exp}} = 110 \mu\text{eV}$ and $\Gamma_{\text{th}} = 110 \mu\text{eV}$, respectively, given in Ref. [3].

The broadening obtained by this shot noise model agrees qualitatively well with the QHAS experimental observations [3]. Note that the broadening described by our model is of the same type as that observed in the spectral lines of gases under high pressure conditions. Moreover, in our simple model the important issue of how the presence of more and more adatoms changes the fields of force felt by the remaining adparticles is not addressed. As far as we know, this problem has not been treated in the literature and certainly merits further investigation. It would be very interesting to know how it affects the broadening of the quasielastic peak. Nevertheless, at the level of the experiments carried out it could happen that the statistical limit (a large number of collisions during the time scales considered) would not lead to any relevant feature, since any effect linked to type of interaction would be blurred up with time.

Regarding the validity of our model, since it is purely stochastic, in principle there are no other limitations than those imposed by realistic physical conditions. For instance, it is clear that the maximum coverage should be $\theta_{\text{Na}} = 1$. However, as the coverage increases, it is also apparent that adsorbate-adsorbate interactions will play a more prominent role in the diffusion dynamics, since in average the motion of each adsorbate will be slowed down and they will feel for longer times the force exerted by their neighbors. In such a case, the Markovian approximation will break down and memory effects should be taken into account. On the other hand, according to Ref. [9] there is experimental evidence that for coverages greater than $\theta_{\text{Na}} = 0.05$, motion perpendicular to the surface is observed, this contributing to the diffusion dynamics. Therefore, one might think that a stochastic model such as ours could at least work fine up to values of the coverage about $\theta_{\text{Na}} = 0.2$ or greater depending on whether QHAS measurements still display effective Lorentzian functions for quasielastic line shapes [3].

Acknowledgments

This work was supported in part by DGICYT (Spain) under project No. FIS2004-02461. R.M.-C. would like to acknowledge the University of Bochum for support from the Deutsche Forschungsgemeinschaft, Contract No. SFB 558. J.L.V. and A.S.S. would like to acknowledge the Spanish Ministry of Education and Science for a grant and a “Juan de la Cierva” contract, respectively. The authors also thank Dr. A. Jardine for interesting discussions and comments.

-
- [1] A. Graham, F. Hofmann, and J.P. Toennies, *J. Chem. Phys.* **104**, 5311 (1996).
 - [2] A.P. Graham, F. Hofmann, J.P. Toennies, L.Y. Chen,

- and S.C. Ying, *Phys. Rev. B* **56**, 10567 (1997).
- [3] J. Ellis, A.P. Graham, F. Hofmann, and J.P. Toennies, *Phys. Rev. B* **63**, 195408 (2001).

- [4] A.P. Jardine, S. Dworski, P. Fouquet, G. Alexandrowicz, D.J. Riley, G.Y.H. Lee, J. Ellis, and W. Allison, *Science* **104**, 1790 (2004); P. Fouquet, A.P. Jardine, S. Dworski, G. Alexandrowicz, W. Allison, and J. Ellis, *Rev. Sci. Instrum.* **76**, 053109 (2005).
- [5] The surface coverage, θ , is defined as the number of adsorbed molecules on a surface divided by the number of molecules in a filled monolayer on that surface.
- [6] J.L. Vega, R. Guantes, and S. Miret-Artés, *J. Phys.: Condens. Matter* **14**, 6193 (2002); **16**, S2879 (2004); S. Miret-Artés and E. Pollak, *ibid.* **17**, S4133 (2005).
- [7] J.M. Sancho, A.M. Lacasta, K. Lindenberg, I.M. Sokolov, and A.H. Romero, *Phys. Rev. Lett.* **92**, 250601 (2004).
- [8] A. Cucchetti and S.C. Ying, *Phys. Rev. B* **60**, 11110 (1999).
- [9] G. Alexandrowicz, A.P. Jardine, H. Hedgeland, W. Allison, and J. Ellis, *Phys. Rev. Lett.* **97**, 156103 (2006).
- [10] D. Frenkel and B. Smit, *Understanding Molecular Simulation* (Academic Press, New York, 2002).
- [11] According to Graham, Toennies, and Benedek [*Surf. Sci. Lett.* **556**, L143 (2004)], for low temperatures the single adsorbate approximation could break due to the presence of organized adsorbate structures mediated by the Lau-Kohn interaction. This type of interaction would be of longer range than the usual lateral dipole-dipole interactions.
- [12] J.H. van Vleck and V.F. Weisskopf, *Rev. Mod. Phys.* **17**, 227 (1945).
- [13] D.A. McQuarrie, *Statistical Mechanics* (Harper and Row, New York, 1976).
- [14] C.W. Gardiner, *Handbook of Stochastic Methods* (Springer-Verlag, Berlin, 1983).
- [15] T. Czernik, J. Kula, J. Luczka, and P. Hänggi, *Phys. Rev. E* **55**, 4057 (1997); J. Luczka, T. Czernik, and P. Hänggi, *ibid.* **56**, 3968 (1997).
- [16] F. Laio, A. Porporato, L. Ridolfi, and I. Rodriguez-Iturbe, *Phys. Rev. E* **63**, 036105 (2001).
- [17] R. Ferrando, M. Mazroui, R. Spadacini, and G.E. Tommei, *New J. Phys.* **7**, 19 (2005).
- [18] P. Hänggi and P. Jung, *Adv. Chem. Phys.* **89**, 239 (1995).
- [19] R. Martínez-Casado, J.L. Vega, A.S. Sanz, and S. Miret-Artés, *Phys. Rev. Lett.* **98**, 19xxxx (2007); e-print arXiv:cond-mat/0702219.
- [20] H. Risken, *The Fokker-Planck Equation* (Springer-Verlag, Berlin, 1984).
- [21] R. Kubo, *Rep. Prog. Phys.* **29**, 255 (1966).
- [22] L. van Hove, *Phys. Rev.* **95**, 249 (1954).
- [23] J.P. Hansen and I.R. McDonald, *Theory of simple liquids* (Academic Press, London, 1986).
- [24] In spin-echo experiments [4, 9] instead of the intermediate scattering function one often calculates the *polarization*, which is the space real (or cosine) Fourier transform of $G(\mathbf{R}, t)$. Nonetheless, both the intermediate scattering function and the polarization provide the same information.
- [25] R. Martínez-Casado, J.L. Vega, A.S. Sanz, and S. Miret-Artés, *J. Phys.: Condens. Matter* **19**, 176006 (2007); e-print arXiv:cond-mat/0608724.
- [26] M.P. Allen and D.J. Tildesley, *Computer Simulation of Liquids* (Clarendon Press, Oxford, 1990).